Journal of Materials Chemistry C

Accepted Manuscript

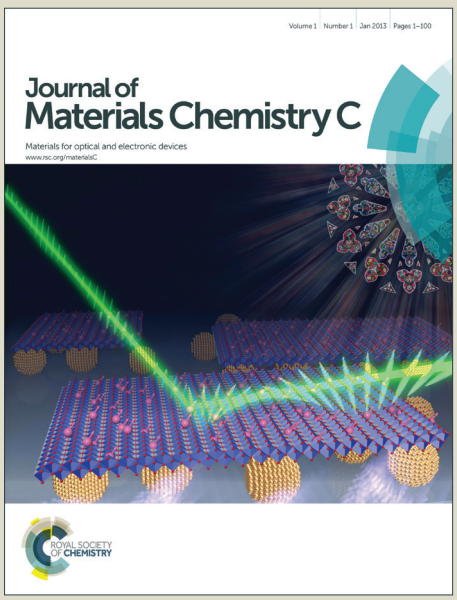

ROYAL SOCIETY OF CHEMISTRY

www.rsc.org/materialsC

Journal Name

ARTICLE

Reduced Thermal Degradation of Red-Emitting $Sr_2Si_5N_8:Eu^{2+}$ Phosphor via Thermal Treatment in Nitrogen

Received 00th January 20xx,
Accepted 00th January 20xx

DOI: 10.1039/x0xx00000x

www.rsc.org/

Chenning Zhang,[a] Tetsuo Uchikoshi,*[a] Rong-Jun Xie,*[b] Lihong Liu,[b] Yujin Cho,[cd] Yoshio Sakka,[a] Naoto Hirosaki[b] and Takashi Sekiguchi[cd]

Red phosphor of $Sr_2Si_5N_8:Eu^{2+}$ was synthesized by a solid state reaction. The as-synthesized phosphor powders were post-treated in N_2 atmosphere. The prepared samples were analyzed by XRD, FE-SEM, TG-DTA, FT-IR, Zeta potential, cathodoluminescence (CL), photoluminescence (PL), quantum efficiencies (QEs), and temperature-dependent PL and QEs techniques. After the thermal treatment in N_2, it was found that the N_2-treatment caused ignored influence on the phase purity and particle morphology; the surface of the phosphor particle became more hydrophilic; the isoelectric point (IEP) of the suspension containing phosphor powder shifted to higher pH value; the edge area (formed surface layer) of the phosphor particle had lower CL intensity than the inner part but it inhibited the surface damage caused by e-beam irradiation; more significantly, the formed surface layer play a passivating role in preventing the Eu^{2+} activator from being oxidized, consequently, effectively reducing the thermal degradation on deteriorating PL intensity of the $Sr_2Si_5N_8:Eu^{2+}$ phosphor.

Introduction

Recently, white light emitting diodes (LEDs) have emerged as an indispensable solid-state light source for next-generation lighting industry and display systems, due to their excellent properties including but not limited to energy savings, environmental-friendliness, downsizing, and durability. Up to now, major challenges in the field of the white LEDs have been focused on achieving high luminous efficacy, high chromatic stability, brilliant color-rending properties, all of which critically rely on the properties of the phosphor used for the white LEDs.[1–3] Generally, enclosing yellow phosphor in blue LED chip is employed to generate white light in LEDs. Although the fabricated white LEDs have high efficiency, its color rendering index (Ra) is still poor. To obtain high Ra, other two alternative approaches are utilized: adding red phosphor into the first approach and combining blue LED diode chip with red and green phosphors,[4, 5] suggesting that the red phosphor plays a key role in improving the color-rending properties of the white LEDs.

$Sr_2Si_5N_8:Eu^{2+}$ is one of the well-known red phosphors as a promising red color component applied in the white LEDs.[3] In the orthorhombic crystal structure of the $Sr_2Si_5N_8$ host (space group Pmn21), the Eu^{2+} ions, activators, occupy the Sr sites in the lattice due to their similar ionic radii. The SiN_4 tetrahedras build up three-dimensional network by corner-sharing N atoms to form a rigid framework, making the phosphor has high chemical and thermal stability.[6] Besides, when excited at 450 nm wavelength, the $Sr_2Si_5N_8:Eu^{2+}$ phosphor gives strong emission in the red region of 616–670 nm with high quantum efficiency.[7, 8]

However, one of the main problems encountered in the red phosphor of $Sr_2Si_5N_8:Eu^{2+}$ is serious thermal degradation on PL property, leading to less reliability and shorter life time of the white LED devices.[9] The origin of the thermal degradation in $Sr_2Si_5N_8:Eu^{2+}$ has recently been reported as the oxidation of Eu ions from divalent to trivalent.[10] The thermal degradation of a phosphor is quite different from its thermal quenching, even though they have similar characteristic; that is, the decrease in PL intensity with increasing temperature. However, the thermal quenching as an intrinsic property of the phosphor relates to the crystal structure, valence band, chemical composition of the host lattice and doping concentration of the activator. Whereas, the thermal degradation as a practical property of the phosphor is caused by extrinsic factors such as humidity, stress, irradiation, and thermal or chemical attacks.[11] Therefore, the thermal quenching is an elastic deformation of luminescence property, but the thermal degradation is a plastic deformation, resulting in that the luminescence intensity cannot recover even by removing the external influences. In this case, how to reduce the influence of thermal degradation on the luminescence property of the $Sr_2Si_5N_8:Eu^{2+}$ phosphor become more significant for the application in the white LEDs.

Passivation, referring to a material becoming “passive”, makes a shielding outer-layer of base material. Currently, the surface passivation as a promising technique has been not only limited in protecting metals or alloys against corrosion, more importantly, but also extended to improve the performance of materials, extensively

[a] Materials Processing Unit, National Institute for Materials Science, Tsukuba, Ibaraki 305-0047, Japan. E-mail: UCHIKOSHI.Tetsuo@nims.go.jp
[b] Sialon Unit, National Institute for Materials Science, Tsukuba, Ibaraki 305-0044, Japan. E-mail: XIE.Rong-Jun@nims.go.jp
[c] Nano-Electronics Materials Unit, National Institute for Materials Science, Tsukuba, Ibaraki 305-0044, Japan
[d] Graduate School of Pure and Applied Science, University of Tsukuba, Tsukuba, Ibaraki 305-0006, Japan
† Footnotes relating to the title and/or authors should appear here.
Electronic Supplementary Information (ESI) available. See DOI: 10.1039/x0xx00000x

in reducing surface recombination in solar cells.[12–17] However, until now, the reports concerning surface passivation have rarely been found in luminescence phosphor, particularly, relating to the thermal degradation property of the phosphor.

In this work, the thermal post-treatment on the as-prepared $Sr_2Si_5N_8:Eu^{2+}$ phosphor was conducted in N_2 atmosphere, with an investigation on the formation of the passivating surface layer around the $Sr_2Si_5N_8:Eu^{2+}$ phosphor affecting on the thermal degradation on its photoluminescence property.

Experimental section

Sample preparation

The $Sr_2Si_5N_8:Eu^{2+}$ phosphor was synthesized by a solid state reaction from reagent grade $SrCO_3$, Eu_2O_3, and Si_3N_4 at 1600 °C for 6 h under an unpressed NH_3 atmosphere. After the reaction, the impurity product of silicate was washed away by acid to obtain the phase-pure $Sr_2Si_5N_8:Eu^{2+}$ phosphor.[18]

The as-prepared $Sr_2Si_5N_8:Eu^{2+}$ powder was packed into an alumina boat and then thermally treated inside a horizontal tube furnace at 300 °C–500 °C in the atmosphere of air or N_2. The heating rate was 5 °C/min and holding time was 3 h. The purity of N_2 was 99.9% and the flow rate was 0.15 L/min.

Characterizations

Phase identification was performed by X-ray diffraction (XRD) on a X-ray diffractometer (model RINT 2200, Rigaku Corp., Tokyo, Japan) with nickel-filtered Cu Kα radiation at 40 kV and 40 mA operation and a scanning speed of 2θ=5° per minute. Particle morphology was observed by a field-emission scanning electron microscopy (FE-SEM) (model S-5000, Hitachi, Ltd., Tokyo, Japan). Thermo gravimetric (TG) and differential thermal analyses (DTA) were performed by a thermometric system (model TG8120, Rigaku Corp., Tokyo, Japan) under N_2/O_2 flow (80% of N_2 and 20% of O_2) in the temperature ranging from 30 °C to 1000 °C at a heating rate of 5 °C/min. Fourier transform infrared (FT-IR) spectra were recorded by a FT-IR spectroscopy (model 4200, JASCO, Tokyo, Japan), with using standard KBr method. To evidence the variation in the surface charge of the phosphor particle after the thermal treatment, the Zeta potential of the phosphor powder dispersed in special grade ethonal (99.5% purity, Nacalai Tesque Inc., Kyoto, Japan) as a function of pH was measured by a zeta potential analyzer (model Zetasizer Nano Z, Malvern Instrument Ltd., Malvern, Worcestershire, UK) and a pH meter (model ss973, Horiba, Ltd., Japan) with a pH electrode (model 6261, Horiba, Ltd., Japan). The pH value of the suspension was adjusted by HCl (0.1mol/L, Kanto, Chemical Co. Inc., Tokyo, Japan) and $NH_3•H_2O$ (10% purity, Wako Pure Chemical Industries, Ltd., Osaka, Japan). Cathodoluminescence (CL) measurement was conducted by an ultrahigh-vacuum SEM equipped with a Gemini electron gun (Omicron, Germany) with an acceleration voltage (electron range) of 5 kV. PL spectra were measured at room temperature by a fluorescent spectrophotometer (model F-4500, Hitachi, Ltd., Tokyo, Japan) with a 200 W Xe-lamp as the excitation source. The excitation spectra were corrected for the spectral distribution of the Xe-lamp intensity by using Rhodamine-B as a reference. The emission spectra were corrected for the spectral response of a monochromator and a photomultiplier tube (model R928P, Hamamatsu, Japan) by a light diffuser and a tungsten lamp (10 V, 4A Noma Electric Corp., New York, USA). Internal and external quantum efficiencies (QEs) were determined by a multichannel photodetector (model MPCD-7000, Otsuka Electronics, Co., Ltd., Osaka, Japan) with a 200 W Xe-lamp as an excitation source. The excitation light from the Xe lamp was filtered by an excitation monochromator (300–600 nm). A white Spectralon standard was illuminated by the resulting monochromatic light for calibration. The reflected light was collected using an integrating sphere. Temperature-dependent PL property was also recorded by the multichannel photodetector, with increasing temperature from 30 °C to 300 °C and decreasing from 300 °C to 30 °C at a heating and cooling rate of 100 °C/min, with 5 min holding time for thermal equilibrium. Temperature-dependent internal and external quantum efficiencies (QEs) were examined by a high sensitivity multichannel photodetector (model MPCD-9800, Otsuka Electronics, Co., Ltd., Osaka, Japan) with a 200 W Xe-lamp as an excitation source. The excitation light from the Xe lamp was also filtered by an excitation monochromator (300–600 nm) and the white Spectralon standard was also used for calibration.

Results and discussion

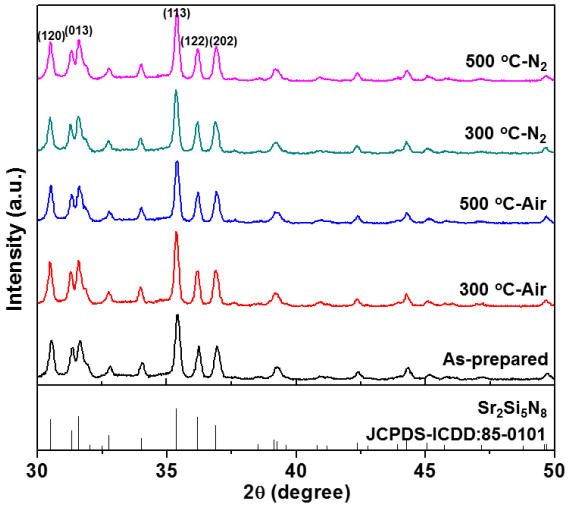

Fig. 1 XRD patterns of the $Sr_2Si_5N_8:Eu^{2+}$ powders including the as-prepared and thermally-treated in air and N_2 at 300–500 °C.

Figure 1 exhibits the XRD patterns of the as-prepared and phosphor powders thermally treated in the air and N_2 atmospheres at 300–500 °C. The main phase of the synthesized sample was identified as $Sr_2Si_5N_8$ that is the host lattice for the prepared phosphor by referring the JCPDS-ICDD database No: 85-0101. After the heating at 300–500 °C, it was observed that the $Sr_2Si_5N_8$ phases were stably kept regardless of the treatment atmospheres, indicating that the heat treatment at 300–500 °C in this study gave ignored effect to the phase variation of the $Sr_2Si_5N_8$. However, it was noticed that the XRD peaks of all the thermally-treated samples slightly shifted to low angle, showing the lattice expansion caused by the thermal treatment.

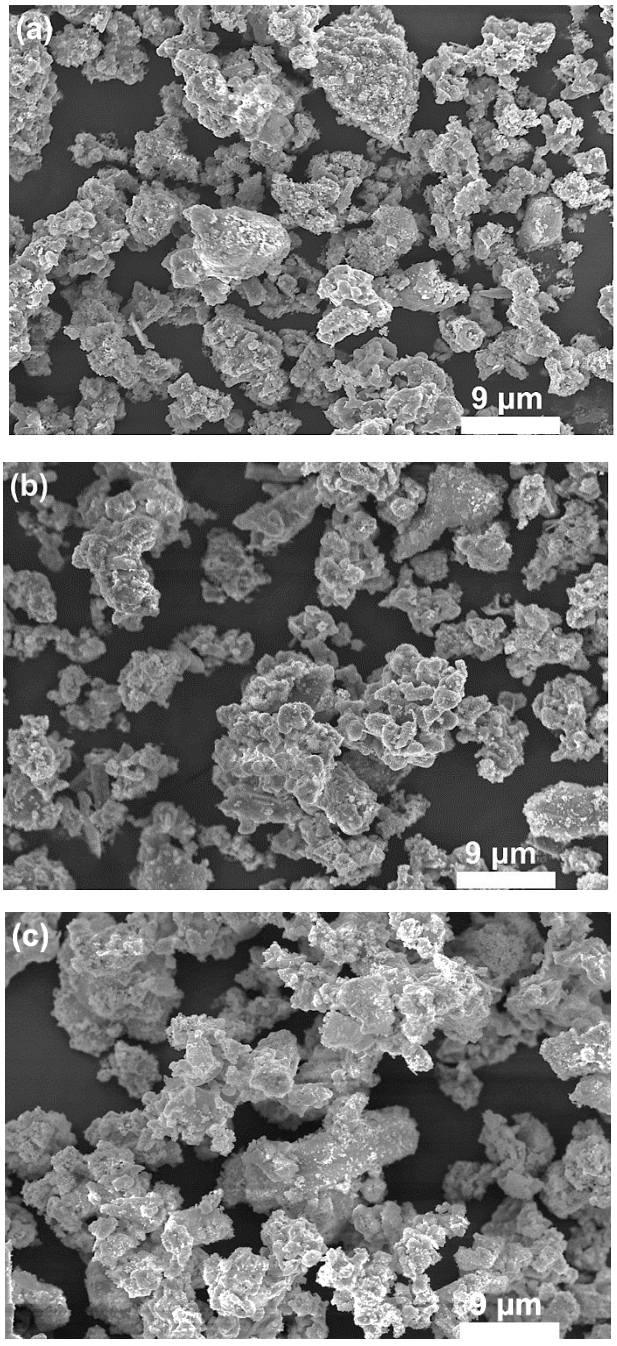

Fig. 2 FE-SEM micrographs of the (a) as-prepared and thermally-treated $Sr_2Si_5N_8:Eu^{2+}$ powders in N_2 at (b) 300 °C and (c) 500 °C.

After extensive FE-SEM observations for all the powders including the as-prepared and heat-treated phosphor powders, no appreciable differences in particle morphology and size were detected for these powders. Figure 2 shows the FE-SEM micrographs of the (a) as-prepared and post-treated $Sr_2Si_5N_8:Eu^{2+}$ powders in N_2 at (b) 300°C and (c) 500°C as typical cases. As seen in Figure 2a, the synthesized $Sr_2Si_5N_8:Eu^{2+}$ powder presented irregular particle shape, with a wide size distribution from several hundreds of nanometers to ~10 μm. In a comparison, after the heat treatments at 300 °C (Figure 2b) and 500 °C (Figure 2c), it was not obviously distinguished that the post-treated powders suffered any influence from the thermal treatments on their particle morphologies.

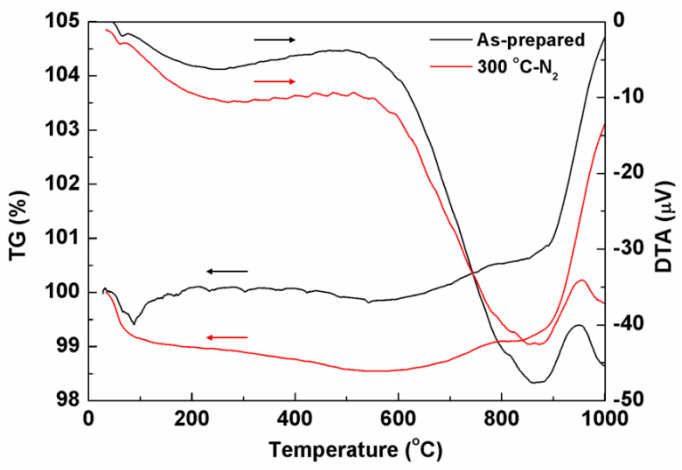

Fig. 3 TG-DTA curves of the as-prepared and 300 °C-N_2 treated $Sr_2Si_5N_8:Eu^{2+}$ powders.

Figure 3 shows the TG-DTA curves of the as-prepared and 300 °C-N_2 treated $Sr_2Si_5N_8:Eu^{2+}$ powders. It can be seen from the TG curves that, after weight loss at ~90 °C ascribed to H_2O desorption, slight weight gain in the as-prepared $Sr_2Si_5N_8:Eu^{2+}$ occurred probably due to phosphor oxidation; appreciable weight gain took place from ~900 °C owing to serious oxidation at high temperature; in contrast, the weight loss in the 300 °C-N_2 treated phosphor ended until ~500 °C; significant weight gain after ~900 °C appeared also as a result of the oxidation. The oxidation was consistently reflected from the exothermic peaks in the DTA curves of the both samples. The different variation tendencies of the TG-DTA curves of both the powders signify that the surface state of the phosphor particle was differentiated after the post-treatment in N_2. The larger amount of H_2O desorption found in the powder thermally treated in N_2 means that the powder surface became more hydrophilic, suggesting the formation of some kind of hydrophilic layer by the treatment, and the lower exothermic peak of the thermal-treated powder indicates that the formed surface layer worked to prevent oxidation of the phosphor powder.

Figure 4 demonstrates the FT-IR spectra of the as-prepared, 300 °C-N_2 treated, and 300 °C-air treated $Sr_2Si_5N_8:Eu^{2+}$ powders. For these 3 samples, the Si-N-Si absorption peaks were assigned to the stretching vibrations at ~472 cm^{-1}, ~926 cm^{-1}, and ~954 cm^{-1};[19] the absorption peaks at ~1630 cm^{-1} and ~2360 cm^{-1} were corresponding to the molecular vibrations of the H_2O and CO_2,[20, 21] respectively, which were both adsorbed on the sample surfaces from air. More significantly, it was found that the shallow absorption bands at ~1404 cm^{-1} were assignable to the Sr/Eu-N bending vibrations for the as-prepared and 300 °C-N_2 treated $Sr_2Si_5N_8:Eu^{2+}$ powders,[22] but that absorption band became strikingly weak in the 300 °C-air treated sample, probably implying that the phosphor encountered serious oxidation after the thermal treatment in air.

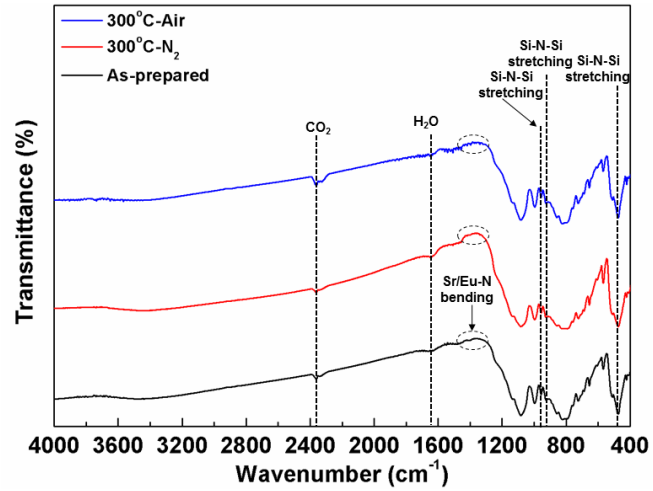

Fig. 4 FT-IR spectra of the as-prepared, 300 °C-N_2, and 300 °C-air treated $Sr_2Si_5N_8:Eu^{2+}$ powders.

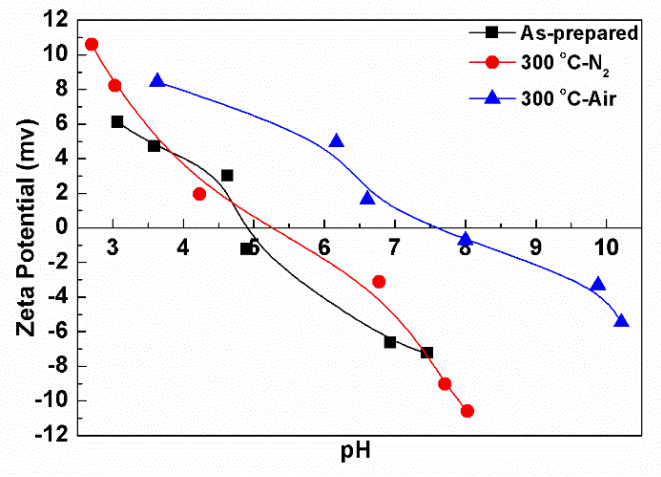

Fig. 5 Zeta potentials of the suspensions containing as-prepared, 300 °C-N_2, and 300 °C-air treated $Sr_2Si_5N_8:Eu^{2+}$ powders as a function of pH.

Zeta potential of the suspensions containing the as-prepared, 300 °C-N_2 treated, and 300 °C-air treated $Sr_2Si_5N_8:Eu^{2+}$ phosphor powders is given in Figure 5. It was found that the IEP, a pH value at which the phosphor particles carry no net electrical charge, of the phosphor powders thermally treated in N_2 and air both shifted towards larger pH value, by comparing with that of the as-prepared sample. The IEP of the as-prepared $Sr_2Si_5N_8:Eu^{2+}$ phosphor was pH_{iep}=~4.9, but it shifted to pH_{iep}=~5.3 after the thermal treatment in N_2 and, more appreciably, it shifted to pH_{iep}=~7.6 after the heat treatment in air. The IEP shift is indicative of the formation of layer around the phosphor particles both via the thermal treatment in N_2 and air. The formed layer was probably oxide compounds like $SrSiO_3$, Sr_2SiO_4, and Sr_3SiO_5,[23] which were generated at the phosphor surface due to the induced oxygen during the post-treatments but could not be detected by the XRD identification on account of extremely small amount of them. For the case of the N_2-treatment, the generations of the oxide compounds were conceived from a viewpoint of the mixture of extremely small amount of air with the used N_2, which was also the reason why the IPE of the 300 °C-N_2 treated sample became slightly larger than that of the as-prepared one but smaller than that of 300 °C-air treated one. Similar report has been found in the literature,[24] in which a passivating oxide layer formed around the fine nickel particles through the heat treatment even though in Ar-dry air mixed gas atmosphere.

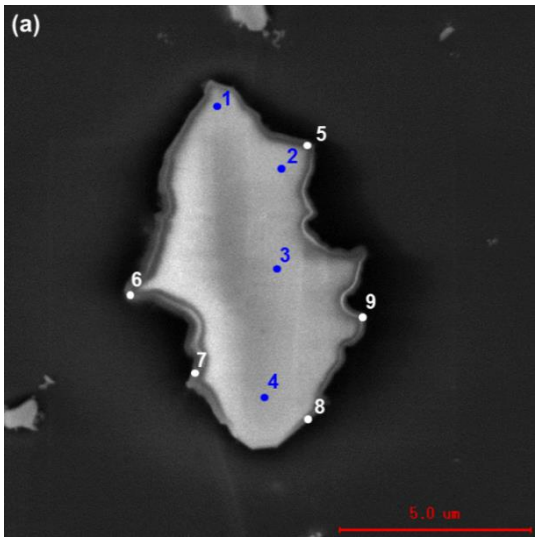

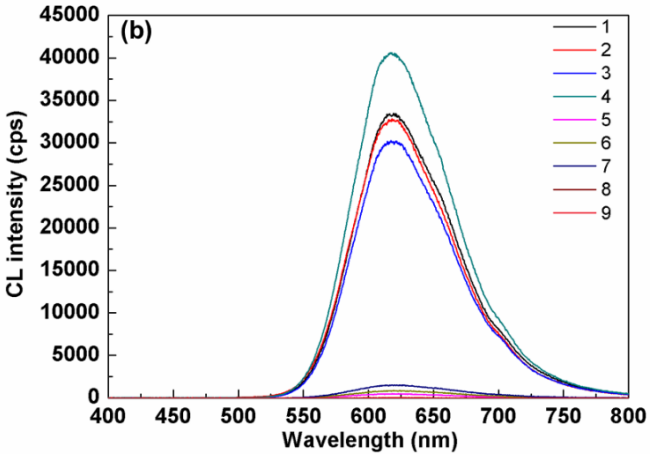

Fig. 6 CL property measured at 9 different points in the cross section of single $Sr_2Si_5N_8:Eu^{2+}$ particle thermally treated at 300 °C in N_2: (a) cross-sectional SEM micrograph and (b) CL spectra.

CL emission is an optical and electromagnetic phenomenon, in which electron beam (e-beam) impacts on a luminescence material to cause visible emission.[25] Currently, CL technique has been widely used to characterize the luminescence properties of phosphor materials; especially, it can independently excite each single phosphor particle.[26–29] Figure 6 exhibits that the cross-sectional CL property measured at 9 different points in single particle of the 300 °C-N_2 treated $Sr_2Si_5N_8:Eu^{2+}$ phosphor: (a) cross-sectional SEM micrograph and (b) CL spectra. From the cross-sectional SEM image

(Figure 6a), it was obviously found that a layer was formed in ~0.2 μm thickness covering around the surface of the post-treated phosphor particle. CL measurement was performed at 9 different points of the N_2-treated $Sr_2Si_5N_8:Eu^{2+}$ particle, in which 4 points were at the inner and the other 5 points were at the edge (newly-formed surface layer) of the particle, as indicated in Figure 6a. As clearly observed from the CL spectra (Figure 6b), all the measured inner points had higher CL intensity that all the examined edge points, implying that the layer that was formed around the phosphor surface after the N_2-treatment had different composition from the host $Sr_2Si_5N_8$. Similar findings have also been reported in decrease in the emission intensities of $Ca_3SiO_4Cl_2:Eu^{2+}$ [30] and $Ca_2BO_3Cl:Eu^{2+}$ [31] phosphors by coating with SiO_2.

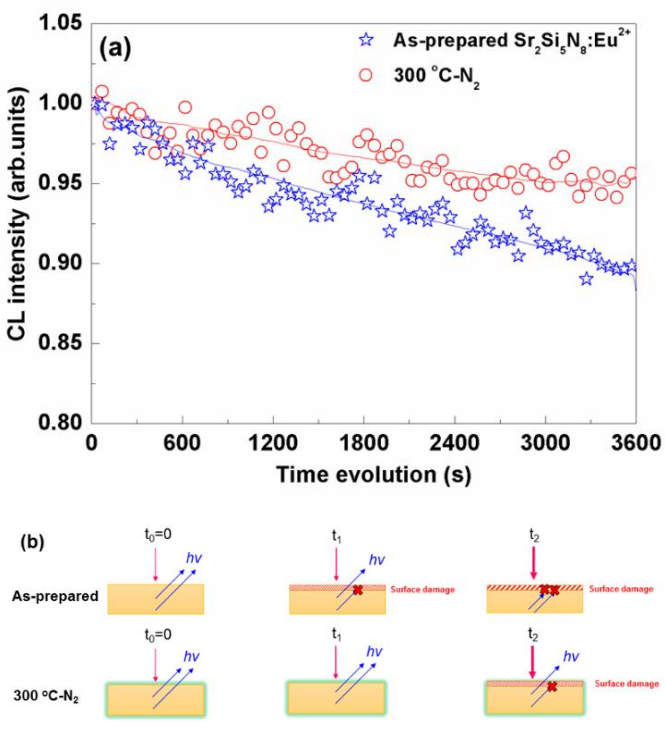

Fig. 7 CL intensity depending on irradiation time evolution for the as-prepared and 300 °C-N_2 treated $Sr_2Si_5N_8:Eu^{2+}$ phosphors: (a) normalized CL spectra and (b) schematic illustration of dependence of CL emission from particle surface on irradiation time.

Figure 7 demonstrates the CL intensity depending on irradiation time evolution for the as-prepared and 300 °C-N_2 treated $Sr_2Si_5N_8:Eu^{2+}$ phosphors: (a) normalized CL spectra and (b) schematic illustration of the dependence of CL emission from particle surface on irradiation time. It was noted that, in Figure 7a, the difference in the variation of the decreased CL intensity of both the samples with prolonging irradiation time was distinctly manifested. Generally, the surface of the phosphor particle is damaged by low-voltage e-beam irradiation and the damage extent becomes more serious with longer irradiation time.[32] In the CL measurement of this work, it can be seen that the CL intensities of the as-prepared and N_2-treated samples became both weaken with evolving irradiation time, however, at t=3600 s of irradiation time, the relative CL intensity of the N_2-heated phosphor was 5% higher than that of the as-prepared one. This phenomenon is reasonably explained from Figure 7b; at 5 kV voltage, with irradiation time evolution, the surface of the as-prepared phosphor was damaged by the e-beam irradiation and turned to be more severe, therefore deteriorating the CL emission from the phosphor surface; in contrast, after the heat treatment in N_2, the formed compound layer around the phosphor surface made a contribution in inhibiting the surface damage that would occurs at the phosphor particles and therefore ensured the CL emit from the particle surface, meanwhile, in turn, confirming the layer formation at the particle surface via the thermal treatment in N_2.

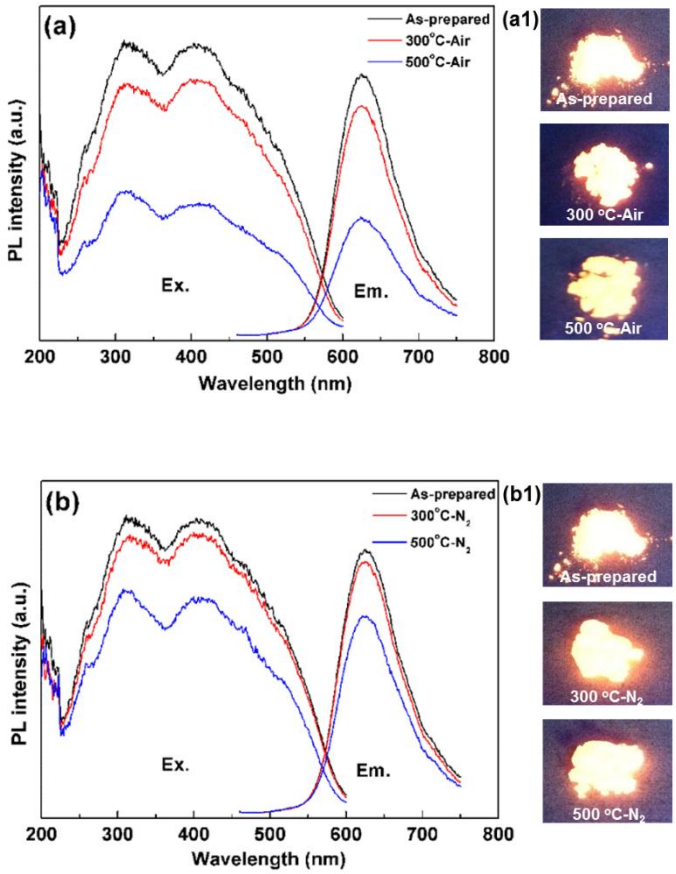

Fig.8 PL spectra of the $Sr_2Si_5N_8:Eu^{2+}$ powders thermally treated in different atmospheres: (a) air, and (b) N_2 in comparison with the PL intensity of the as-prepared phosphor. Excitation spectra monitored at 625 nm and emission spectra excited under 405 nm. The insets are the photographs of the (a1) thermal treated in air and (b1) in N_2 phosphor powders excited inside a 365 nm-UV box.

Figure 8 displays the PL spectra of the post-treated $Sr_2Si_5N_8:Eu^{2+}$ powders at 300°C–500 °C in various atmospheres: (a) air and (b) N_2 in comparison with that of the as-prepared phosphor. The excitation spectra were monitored at 625 nm and emission spectra were excited under 405 nm. In Figure 8a, the emission intensity of the air-treated powder declined by ~12% after 300 °C-treatment in air and

dropped by ~54% after 500 °C-treatment. The declined PL emission intensity with increasing heating temperature in air can be clearly perceived from the different brightness under the UV irradiation in the inset of Figure 8a. The degradation in the PL intensity should be considered by both oxidations of the activator Eu^{2+} and $Sr_2Si_5N_8$:Eu^{2+} host lattice, involving: (1) the activator Eu^{2+} being oxidized into Eu^{3+}. Based on the kinetic of the oxidation reaction proposed by Bizarri et al.,[33] the degraded PL intensity after the heat treatment in air may be due to three different steps leading to the oxidation of the Eu^{2+} ions: (i) the adsorption of the gaseous oxygen atom into an oxygen vacancy of the $Sr_2Si_5N_8$:Eu^{2+} phosphor lattice; (ii) owing to the increased temperature during the thermal treatment, the adsorbed oxygen atom diffused into the conduction layer of the europium ions; and (iii) the electronic transfer from the Eu^{2+} ions to the adsorbed oxygen when the two species are close to each other. The oxidation process is expressed by the following equation:

$$2Eu^{2+} + \frac{1}{2}O_2(g) + V_O^{\cdot\cdot} \rightarrow 2Eu^{3+} + O_O^{\times} \quad (1)$$

where Eu^{2+} is the divalent europium ion, $O_2(g)$ is the gaseous oxygen atom, $V_O^{\cdot\cdot}$ is the oxygen vacancy, Eu^{3+} is the trivalent europium, and $O_O^{\times}$ is the oxygen ion of the lattice, "•" and "×" are the Kröger-Vink notations for the net charge +1 and the zero net charge, respectively; and (2) the $Sr_2Si_5N_8$ host at the particle surface being oxidized after the heat treatment to form some compounds such as $SrSiO_3$, Sr_2SiO_4, and Sr_3SiO_5 as revealed by the IEP variation (Figure 5). In the literature,[34] it also reported similar reason for moisture-induced degradation on PL intensity, which was explained by the phosphor host and activator oxidations via an oxidant-gas penetration mechanism. Whereas, from the PL spectra of the phosphor powders heated in N_2 atmosphere (Figure 8b), it was found that the emission intensity of the N_2-heated sample slightly decreased by ~4.8% at 300 °C-processing and ~25% at 500 °C-processing, unlike the case of serious decrease in PL intensity after the air-treatment. The difference in the brightness appearances under the UV irradiation of the phosphor powders thermally treated in air and in N_2 can be unambiguously observed from the insets in Figure 8a and Figure 8b. The slightly decreased PL intensity is attributed to the retard on the oxidation of Eu^{2+} activator and $Sr_2Si_5N_8$ host by the thermal treatment in N_2.

Figure 9 exhibits the variation of external and internal QEs (η_{ex} and η_{in}) of the heated-treated $Sr_2Si_5N_8$:Eu^{2+} powders in air and N_2 as a function of the treatment temperature. The η_{ex} and η_{in} were calculated using the following equations:[35]

$$\eta_{ex} = \frac{\int \lambda P(\lambda) d\lambda}{\int \lambda E(\lambda) d\lambda} \quad (2)$$

$$\eta_{in} = \frac{\int \lambda P(\lambda) d\lambda}{\int \lambda [E(\lambda) - R(\lambda)] d\lambda} \quad (3)$$

where $E(\lambda)/h\upsilon$, $R(\lambda)/h\upsilon$, and $P(\lambda)/h\upsilon$ are the numbers of photons in the excitation, reflectance, and emission spectra of the phosphor, respectively. The η_{ex} and η_{in} of the heat-treated powders both decreased with increasing treatment temperature, irrespective of the air or N_2 treatment atmosphere. However, it was comparably noted that the η_{ex} and η_{in} of the N_2-treated sample much slowly declined with increasing treatment temperature in contrast to those of the air-treated one. This different variation tendency was also explained by the contribution of N_2-treatment in inhibiting the oxidations of the activator Eu^{2+} ions and host $Sr_2Si_5N_8$, which has been known from the PL spectra (Figure 8).

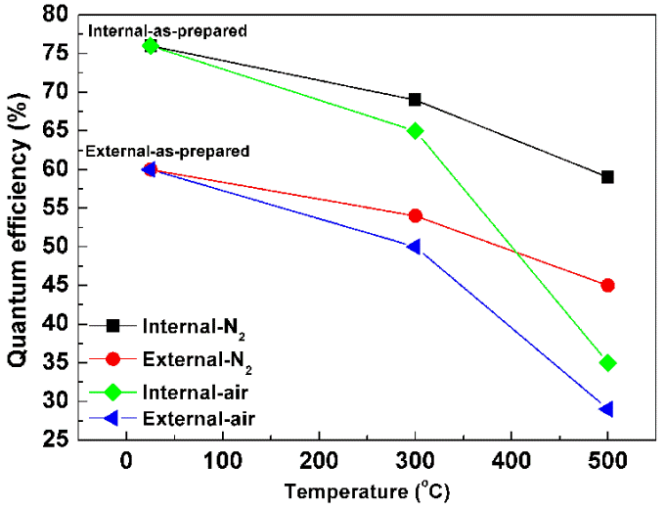

Fig.9 Variation of internal and external QEs of the $Sr_2Si_5N_8$:Eu^{2+} powders thermally treated in air and N_2 as a function of heating temperature.

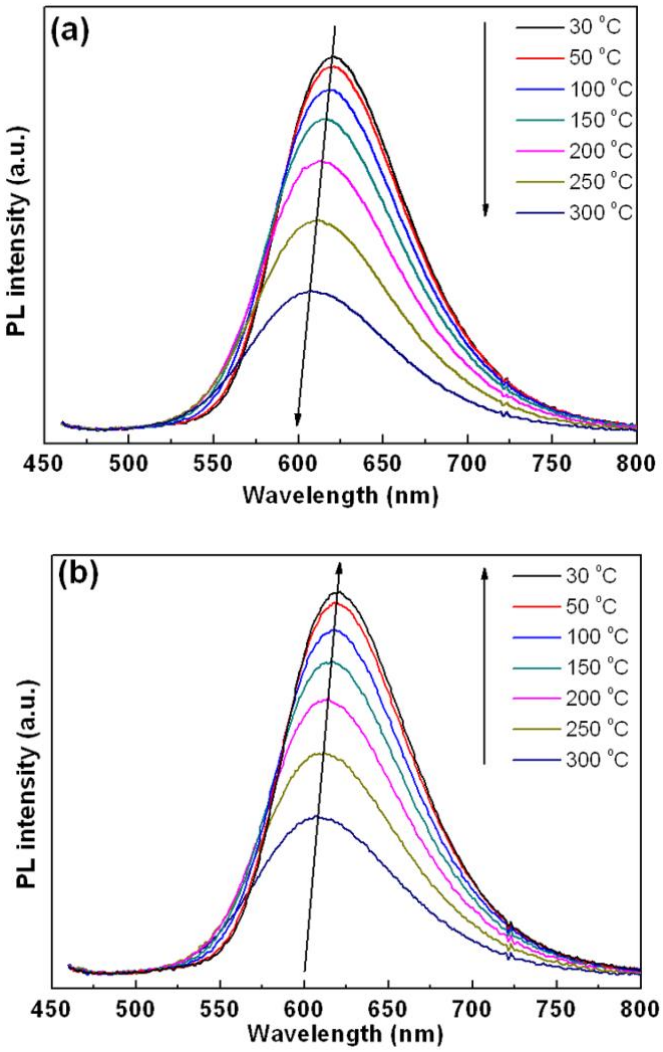

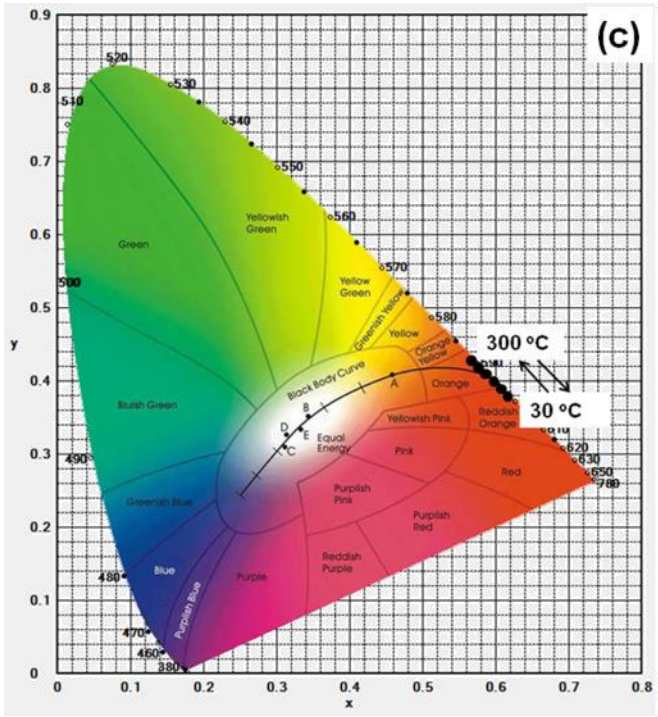

Fig.10 Temperature-dependent PL spectra of the as-prepared $Sr_2Si_5N_8:Eu^{2+}$ phosphor: (a) heating from 30 °C to 300 °C, (b) cooling from 300 °C to 30 °C, and (c) diagram of chromaticity coordinates depending on temperature.

Temperature-dependent PL spectra of the as-prepared $Sr_2Si_5N_8:Eu^{2+}$ phosphor: (a) heated from 30 °C to 300 °C, (b) cooled from 300 °C to 30 °C, and (c) diagram of chromaticity coordinates depending on the temperature, are given in Figure 10. It was obviously found that the blue shift of wavelength took place in the emission peak (Figure 10a) with heating temperature from 30 °C to 300 °C; while, the red shift occurred in the emission wavelength (Figure 10b) with cooling from 300 °C to 30 °C. Consequently, the chromaticity coordinate for the color appearance of the sample was varied from reddish orange at 30 °C to orange at 300 °C with heating temperature and recovered to reddish orange when decreasing temperature to 30 °C (Figure 10c). Moreover, the phenomenon of the wavelength shift of emission peak with heating and cooling temperatures was also found in all the phosphors thermally-treated in air and N_2. The dependence of the emission wavelength shift on the temperature should be considered as below: in this study, the heating temperature lifted up the lowest 5d energy level of the activator Eu^{2+} but the cooling temperature lowered it down. Generally, luminescence is defined as that the electrons return to the ground state by spontaneous emission of photons after they are promoted into excited states by absorbing photons with appropriate frequency.[36] For the $Sr_2Si_5N_8:Eu^{2+}$ phosphor, when electrons absorbed energy under the 405 nm excitation, they transited to the $4f^65d^1$ excited state of Eu^{2+} by forming valence electrons in the excited state and leaving behind holes in the $4f^7$ ground state. When the electron dropped down to recombine the holes, this process gave rise to the photon emission. Moreover, this luminescence process is usually corresponding to the transitions between the lowest excited level and the ground state,[37] since degenerate 5d levels is lifted by non- spherical electrostatic interaction with surrounding ions so that resulted in two or more levels.[38] In this work, the lowest 5d energy level of the excited state was lifted or lowered by the thermal induction of heating or cooling temperature, therefore leading to the emission at a shorter (blue shift) or longer (red shift) wavelength.[39] In addition, it has been reported that the Eu^{2+} dopants replaced two Sr^{2+} in the host lattice because the ionic radii of Sr^{2+} (1.26 and 1.31 Å) slightly differed from Eu^{2+} (1.25 and 1.30 Å), respectively.[10, 40] Thus, the different Sr positions have different accommodation situations, including loose and tight sites for the Eu^{2+} activator to form different crossing points, which are corresponding with higher-energy (shorter-wavelength) and lower-energy (longer-wavelength) emissions, respectively.[41, 42] This suggests that the heating temperature favored the excited electron easily transfer from the 5d level to the 4f ground state via the cross point through the loose site accommodation.

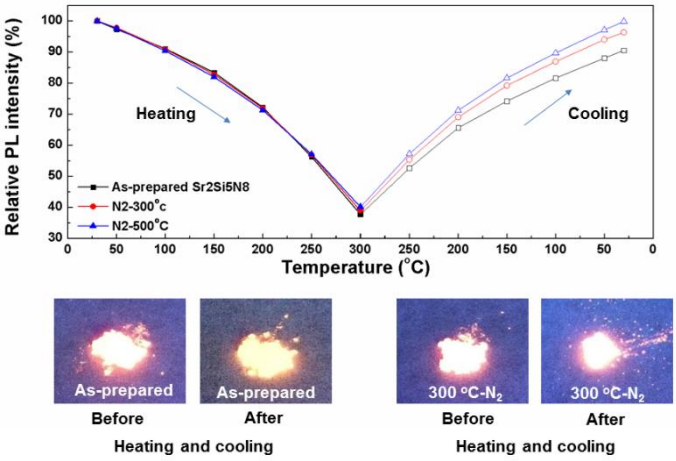

Fig.11 Relative PL intensities of the as-prepared and N_2-treated $Sr_2Si_5N_8:Eu^{2+}$ phosphors with heating (heating from 30 °C to 300 °C) and cooling (from 300 °C to 30 °C) to indicate the influence of thermal degradation on PL intensity. The insets are the photograph of the as-prepared and 300 °C-N_2 treated phosphor powders excited in a 365 nm-UV box before and after heating and cooling processes when determining thermal degradation property.

Recovery of relative PL intensity of the phosphor when heating up from 30 °C to 300 °C and then cooling down from 300 °C to 30 °C was used to indicate the influence of thermal degradation on PL intensity. Figure 11 gives the relative PL intensity of the as-prepared and N_2-treated $Sr_2Si_5N_8:Eu^{2+}$ phosphors depending on heating and cooling temperatures. For the as-prepared $Sr_2Si_5N_8:Eu^{2+}$, the recovered relative PL intensity of the phosphor after heating up to 300 °C and then cooling down to 30 °C was 90.5% of the initial intensity. In comparison, the recovered relative PL intensity of the N_2-treated phosphor was significantly improved: 96.3% of the initial intensity under 300 °C-treatment and 99.8% under 500 °C-treatment, indicating that the thermal-treatment in N_2 as a post-treatment way

reduced the influence of the thermal degradation on PL intensity, which can be comparably distinguished by the brightness variation of the as-prepared and N_2-treated phosphor powders in a 365 nm-UV box before and after heating and cooling processes from the inset of Figure 11. Furthermore, the contribution of the thermal-treatment in N_2 on decreasing the thermal degradation on PL intensity can also be more accurately found in the temperature-dependent external and internal QEs of the as-prepared and 300 °C-N_2 treated $Sr_2Si_5N_8:Eu^{2+}$ phosphors with heating (from 50 °C to 300 °C) and cooling (from 300 °C to 50 °C) temperature, as shown in Figure 12. When temperature cooling down to 50 °C, the recovered external and internal QEs of the 300 °C-N_2 treated phosphor were 99.5% and 99.8% appreciably higher that those of 92.7% and 94.1% of the as-prepared $Sr_2Si_5N_8:Eu^{2+}$, respectively.

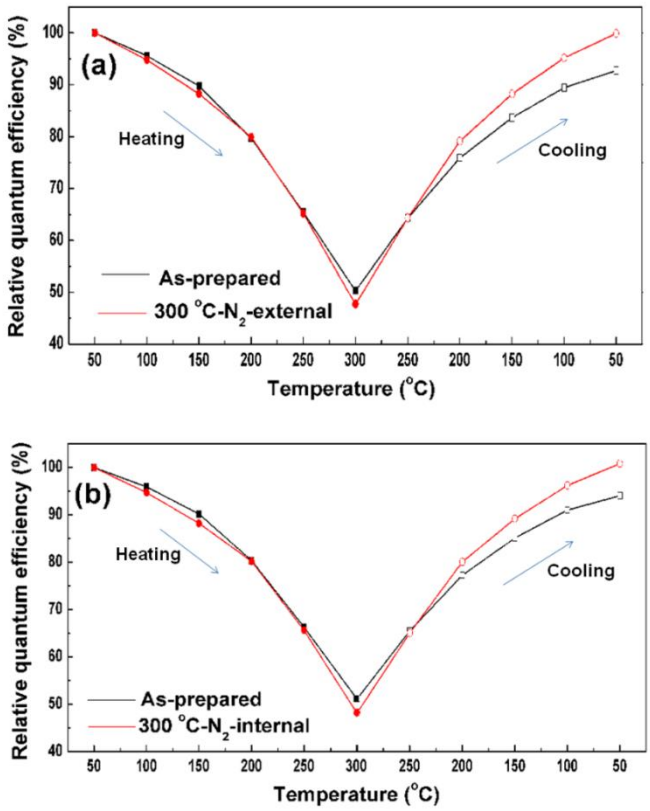

Fig.12 Temperature-dependent external and internal QEs of the as-prepared and 300 °C-N_2 treated $Sr_2Si_5N_8:Eu^{2+}$ phosphors with heating (from 50 °C to 300 °C) and cooling (from 300 °C to 50 °C) temperature to indicate the influence of thermal degradation on PL intensity.

The main reason for the thermal degradation on deteriorating PL intensity of the $Sr_2Si_5N_8:Eu^{2+}$ phosphor should be mainly attributed to the oxidation of the Eu^{2+} activator. Figure 13 illustrates the crystal structure of $Sr_2Si_5N_8:Eu^{2+}$. It can be seen that the Eu^{2+} activator in the $Sr_2Si_5N_8$ structure is inserted between the [SiN_4] tetrahedral layers, enabling Eu^{2+} easily contact with O_2 although the network of vertex-sharing [SiN_4] tetrahedral connects two ($N^{[2]}$) and three ($N^{[3]}$) neighboring Si atoms to form a rigid and stable structure. Similar case has been reported in the crystal structure of $BaMgAl_{10}O_{17}:Eu^{2+}$ phosphor, in which the Eu^{2+} ions are also inserted between the conduction layers and therefore Eu^{2+} is readily exposed to O_2.[43] In addition, thermally stable luminescence has been proposed in Eu^{2+}-doped $Ba_2Ln(BO_3)_2Cl$ (Ln=Y, Gd, and Lu) phosphors due to different Eu^{2+} ion sites substituting Ba^{2+} positions.[44]

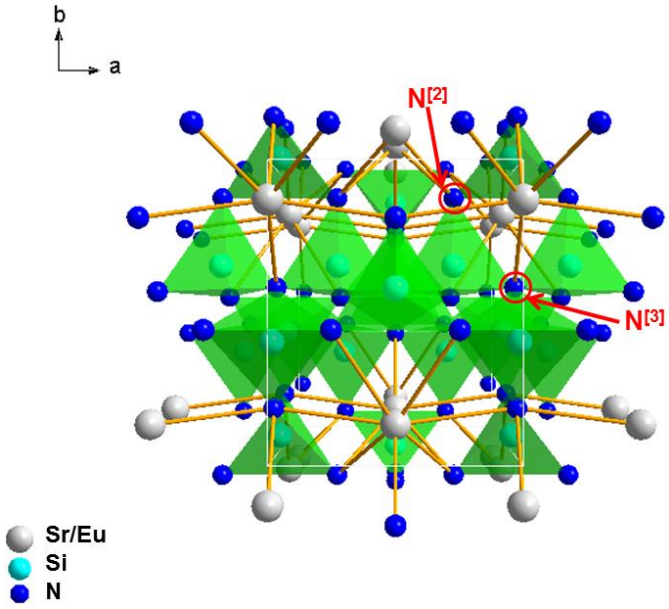

Fig.13 Crystal structure of $Sr_2Si_5N_8:Eu^{2+}$, viewing along *c*-axis.

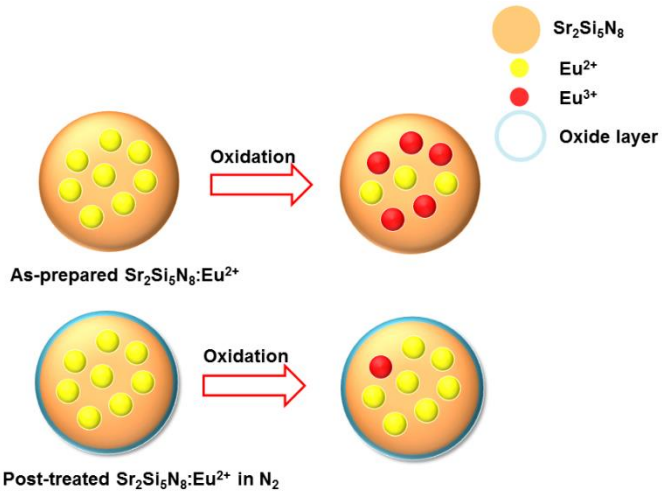

Fig. 14 Schematic illustration of contribution of oxide compound layer formed around $Sr_2Si_5N_8:Eu^{2+}$ surface via thermal treatment in N_2 in preventing activator Eu^{2+} ions from being oxidized.

In addition, the higher covalence of Sr–N than that of Sr–O in the $Sr_2Si_5N_8:Eu^{2+}$ structure also makes Eu^{2+} have a higher probability to connect with O_2.[33] However, the reduction in the thermal degradation on PL intensity by the thermal treatment in N_2, as revealed in Figure 11 and Figure 12, indicates that the oxidation of Eu^{2+} was significantly inhibited by this post treatment. This

phenomenon should be understood from that the formation of the oxide compound layer around the surface of the $Sr_2Si_5N_8:Eu^{2+}$ phosphor after the heat-treatment in N_2 played a role as a passivation layer in avoiding O_2 attack on the Eu^{2+} activator and preventing O_2 from penetrating into the inner of the phosphor, as illustrated in Figure 14, and, as a result, the formed passivation layer reduced the influence of the thermal degradation on deteriorating PL intensity of the phosphor.

Conclusions

Red phosphor of $Sr_2Si_5N_8:Eu^{2+}$ was synthesized by a solid state reaction. The thermal post-treatment was conducted on the as-prepared phosphor powders at 300 °C–500 °C in N_2 atmospheres. The N_2-treatment caused ignored influence on the phase purity and particle morphology of the phosphor powders. After the heat treatment in N_2, there were some changes occurring in the phosphor: the surface of the phosphor particle became more hydrophilic; the isoelectric point of the suspension of the phosphor powder shifted to higher pH value; the formed surface layer around the phosphor particle had lower CL intensity than the inner part but it inhibited the surface damage caused by e-beam irradiation. The Eu^{2+} activator and the $Sr_2Si_5N_8$ host after the heat treatment in air were seriously oxidized, which was known from dramatically deteriorated PL property; in comparison, these oxidation were effectively retarded via the thermal treatment in N_2. In addition, the blue or red shift in the emission peak of the phosphor was found to be varied with temperature increase or decrease. More interestingly, the heat treatment in N_2 significantly depressed the influence of the thermal degradation on the PL intensity of the $Sr_2Si_5N_8:Eu^{2+}$ phosphor through the formation of the passivating layer around the phosphor particle against the activator Eu^{2+} being oxidized, suggesting an effectively improved possibility in application for the white LEDs.

Acknowledgements

The authors are grateful to Dr. Tohru Suzuki in National Institute for Materials Science (NIMS) for TG-DTA equipment training, Dr. Ji-guang Li in NIMS for FT-IR analysis support, and Dr. Benjamin Dierre in NIMS for suggestion on CL measurements. Rong-Jun Xie acknowledges the JSPS KAKENHI (no. 23560811) and the National Natural Science Foundation of China (no. 51272259).

Notes and references

1. S. Ye, F. Xiao, Y. X. Pan, Y. Y. Ma, and Q. Y. Zhang, *Mat. Sci. Eng. R*, 2010, **71**, 1–34.
2. N. C. George, K. A. Denault and R. Seshadri, *Annu. Rev. Mater. Res.*, 2013, **43**, 481–501.
3. R.-J. Xie and N. Hirosaki, *Sci. Technol. Adv. Mat.*, 2007, **8**, 588–600.
4. L. Chen, C. C. Lin, C. W. Yeh and R. S. Liu, *Materials*, 2010, **3**, 2172–2195.
5. R.-J. Xie, N. Hirosaki, Y. Q. Li and T. Takeda, *Materials*, 2010, **3**, 3777–3793.
6. T. Schlieper, W. Milius and W. Schnick, *Z. Anorg. Allg. Chem.*, 1995, **621**, 1380–1384.
7. Y. Q. Li, J. E. J. van Steen, J. W. H. van Krevel, G. Botty, A. C. A. Delsing, F. J.; de With, G. DiSalvo and H. T. Hintzen, *J. Alloy. Compd.*, 2006, **417**, 273–279.
8. R.-J. Xie, N. Hirosaki, T. Suehiro, F. F. Xu and M. Mitomo, *Chem. Mater.*, 2006, **18**, 5578–5583.
9. R.-J. Xie, N. Hirosaki, T. Takeda and T. Suehiro, *ECS J. Solid State Sc.*, 2013, **2**, R3031–R3040.
10. C. W. Yeh, W. T. Chen, R. S. Liu, S. F. Hu, H. S. Sheu, J. M. Chen and H. T. Hintzen, *J. Am. Chem. Soc.*, 2012, **134**, 14108–14117.
11. C. Y. Wang, R.-J. Xie, F. Li and X. Xu, *J. Mater. Chem. C*, 2014, **2**, 2735–2742.
12. A. G. Aberle, *Prog. Photovoltaics*, 2000, **8**, 473–487.
13. C.-F. Chi, P. Chen, Y.-L. Lee, I. P. Liu, S.-C. Chou, X.-L. Zhang and U. Bach, *J. Mater. Chem.*, 2011, **21**, 17534–17540.
14. D. Wang, S. Hou, H. Wu, C. Zhang, Z. Chu and D. Zou, *J. Mater. Chem.*, 2011, **21**, 6383–6388.
15. W.-C. Wang, C.-W. Lin, H.-J. Chen, C.-W. Chang, J.-J. Huang, M.-J. Yang, B. Tjahjono, J.-J. Huang, W.-C. Hsu and M.-J. Chen, *ACS Appl. Mater. Inter.*, 2013, **5**, 9752–9759.
16. M. Z. Rahman, *Renew. Sust. Energ. Rev.*, 2014, **30**, 734–742.
17. F. Wang, X. Zhang, L. Wang, Y. Jiang, C. Wei, J. Sun and Y. Zhao, *ACS Appl. Mater. Inter.*, 2014, ***6***, 15098–15104.
18. R.-J. Xie, N. Hirosaki, N. Kimura, K. Sakuma and M. Mitomo, *Appl. Phys. Lett.*, 2007, **90**, 191101.
19. M. I. Baraton, W. Chang and B. H. Kear, *J. Phys. Chem.*, 1996, **100**, 16647–16652.
20. H. A. Al-Abadleh and V. H. Grassian, *Langmuir*, 2003, **19**, 341–347.
21. F. Fleyfel and J. P. Devlin, *J. Phys. Chem.*, 1989, **93**, 7292–7294.
22. L. C. Ju, X. Xu, L. Y. Hao, Y. Lin and M. H. Lee, *J. Mater. Chem. C*, 2015, **3**, 1567–1575.
23. Y. Kim, J. Kim and S. Kang, *J. Mater. Chem. C*, 2013, **1**, 69–78.
24. T. Uchikoshi, Y. Sakka, M. Yoshitake and K. Yoshihara, *NanoStruct. Mater.*, 1994, **4**, 199–206.
25. B. G. Yacobi and D. B. Holt, *Cathodoluminescence Microscopy of Inorganic Solids*, Plenum, New York, 1990.
26. X. M. Liu, L. S. Yan and J. Lin, *J. Phys. Chem. C*, 2009, **113**, 8478–8483.
27. Y. T. Han, X. Wu, G. Z. Shen, B. Dierre, L. H. Gong, F. Y. Qu, Y. Bando, T. Sekiguchi, F. Filippo and D. Golberg, *J. Phys. Chem. C*, 2013, **114**, 8235–8240.
28. B. D. Liu, Y. Bando, B. Dierre, T. Sekiguchi, D. Golberg and X. Jiang, *ACS Appl. Mater. Inter.*, 2013, **5**, 9199–9204.
29. F. Yuan, B. D. Liu, Z. E. Wang, B. Yang, Y. Yin, B. Dierre, T. Sekiguchi, G. F. Zhang and X. Jiang, *ACS Appl. Mater. Inter.*, 2010, **5**, 12066–12072.
30. J. Q. Zhuang, Z. G. Xia, H. K. Liu, Z. P. Zhang and L. B. Liao, *Appl. Surf. Sci.,* 2011, **257**, 4350–4353.
31. H. K. Liu, Z. G. Xia, J. Q. Zhuang, Z. P. Zhang and L. B. Liao, *J. Phys. Chem. Solids,* 2012, **73**, 104–108.
32. S. Itoh, T. Kimizuka and T. Tonegawa, *J. Electrochem. Soc.*, 1989, **136**, 1819–1823.
33. G. Bizarri and B. Moine, *J. Lum.*, 2005, **113**, 199–213.
34. J. Zhu, L. Wang, T. Zhou, Y. Cho, T. Suehiro, T. Takeda, M. Lu, T. Sekiguchi, N. Hirosaki and R.-J. Xie, *J. Mater. Chem. C*, 2015, **3**, 3181–3188.
35. K. Ohkubo and T. Shigeta, *J. Illum. Engng. Inst. Jpn.*, 1999, **83**, 87–93.
36. J I. Pankove, *Optical processes in semiconductors*. Courier Dover Publications, New York 2012.
37. G. Blasse and B. C. Grabmaier, *Luminescent materials.* Springer, Berlin 1994.
38. K H J. Buschow and F R. de Boer, *Physics of Magnetism and Magnetic Materials.* Springer: New York, 2003.
39. W. Y. Li, R.-J. Xie, T. L. Zhou, L. H. Liu and Y. J .Zhu, *Dalton T.*, 2014, **43**, 6132–6138.
40. R. D. Shannon, *Acta Crystallogr. A*, 1976, **32**, 751–767.

41. K. S. Sohn, B. Lee, R.-J. Xie and N. Hirosaki, *Opt. Lett.*, 2009, **34**, 3427–3429.
42. K. S. Sohn, S. Lee, R.-J. Xie and N. Hirosaki, *Appl. Phys. Lett.*, 2009, **95**, 121903.
43. K. B. Kim, Y. I. Kim, H. G. Chun, T. Y. Cho, J. S. Jung and J. G. Kang, *Chem. Mater.*, 2002, **14**, 5045–5052.
44. Z. G. Xia, X. M. Wang, Y. X. Wang, L. B. Liao and X. P. Jing, *Inorg. Chem.,* 2011, **50**, 10134–10142.

A table of contents entry

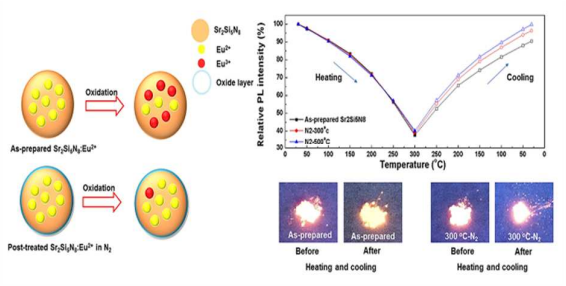

Thermal degradation of $Sr_2Si_5N_8$:Eu^{2+} phosphor reduced by formation of passivation surface layer around phosphor particle contributing in inhibiting Eu^{2+} oxidation